JBC RESEARCH ARTICLE

Viperin expression leads to downregulation of mitochondrial genes through misincorporation of ddhCTP by mitochondrial RNA polymerase

Received for publication, December 13, 2024, and in revised form, February 18, 2025 Published, Papers in Press, February 25, 2025,
https://doi.org/10.1016/j.jbc.2025.108359

Srijoni Majhi[1,‡], **Pronay Roy**[1,‡], **Minshik Jo**[1], **Jiying Liu**[1], **Rebecca Hurto**[2], **Lydia Freddolino**[2], and **E. Neil G. Marsh**[1,2,*]

From the [1]*Department of Chemistry, University of Michigan;* [2]*Department of Biological Chemistry, University of Michigan Medical School, Ann Arbor, Michigan, USA*

Reviewed by members of the JBC Editorial Board. Edited by Craig Cameron

Increasing lines of evidence link the expression of the interferon-stimulated gene *RSAD2*, encoding the antiviral enzyme, viperin, to autoimmune disease. Autoimmune diseases are characterized by chronic overproduction of cytokines such as interferons that upregulate the inflammatory response. Immune cells exposed to interferon selectively downregulate transcription of the mitochondrially encoded components of the oxidative phosphorylation system, which leads to mitochondria becoming dysfunctional and impairing their ability to produce ATP. But the mechanism by which downregulation occurs has remained unknown. Here we show that 3′-deoxy-3′,4′-didehydrocytidine triphosphate (ddhCTP) which is synthesized by viperin suppresses mitochondrial transcription by causing premature chain termination when misincorporated by the mitochondrial RNA polymerase (POLRMT). We show that viperin expression in human cell lines downregulates mitochondrially encoded gene expression. A similar effect is observed across multiple cell lines when cells are exposed to ddhC, the precursor to ddhCTP. The pattern of gene downregulation fits well with a simple, quantitative model describing chain-termination. *In vitro* measurements with purified POLRMT demonstrate that ddhCTP competes effectively with CTP, leading to its misincorporation into RNA. These findings reveal a new molecular mechanism for mitochondrial transcriptional regulation that explains the reduction in mitochondrially-encoded transcript levels in response to chronic interferon stimulation, characteristic of inflammatory diseases.

In addition to generating ATP, mitochondria are now known to play a central role in many other cellular processes; these include regulating cellular calcium levels, programmed cell death (apoptosis), and the innate immune response (1, 2). Consequently, mitochondrial dysregulation and/or metabolic reprograming is linked to many diseases (3), including cancer, diabetes, Alzheimer's, and autoimmune diseases such as rheumatoid arthritis (RA), Sjogren's syndrome, and systemic lupus erythematosus (SLE) (4–7). The chronic inflammatory response characteristic of autoimmune diseases and many cancers is known to cause dysregulation or reprogramming of mitochondrial metabolism (4). In response to cellular stress, mitochondrial DNA (mt-DNA) is released into the cytosol where it triggers the transcription of cytokines such as IFNs through the TLR9/NF-κB, cGAS-STING, MDA5/MAVS, and inflammasome signaling pathways (5). This positive feedback loop is thought to play an important role in pro-inflammatory diseases such as SLE (7) and RA (5).

The transcription of mitochondrially encoded genes (mt-genes) in immune cells is significantly attenuated in inflammatory diseases, leading to impaired mitochondrial respiratory function (5). For example, $CD4^+$ and $CD8^+$ T cells from SLE patients with a high IFN signature were found to have downregulated mt-genes in oxidative phosphorylation (OXPHOS), whereas nuclear-encoded genes for mitochondrial proteins were unaffected (8, 9). Downregulation of mt-genes is linked to the chronic exposure of cells to IFNs that are produced as part of the inflammatory cascade. Indeed, IFN-induced downregulation of mt-genes, leading to decreased cellular respiration and a reduction in ATP levels, was first demonstrated in a human B cell line some 30 years ago (10, 11). However, due in part to the complexity of the IFN response—hundreds of genes are currently known to be regulated by IFNs (12)—the mechanism of downregulation has remained unexplained.

RSAD2 (a.k.a. *cig5*) is one of the most highly upregulated IFN-stimulated genes (ISGs) (13). *RSAD2* encodes the antiviral protein, viperin (Virus Inhibitory Protein Endoplasmic Reticulum-associated Interferon inducible). Viperin is an ancient enzyme that is present in all kingdoms of life and one of the very few radical SAM enzymes found in humans (14–16). It synthesizes the antiviral nucleotide 3′-deoxy-3′,4′-didehydro-CTP (ddhCTP) by dehydration of CTP through a radical-mechanism (17). In higher eukaryotes viperin is integral to the innate immune response (18): its expression is induced by type-I IFN and IFN-γ through the JAK-STAT signaling pathway (Fig. 1), and by stimulation of the (RIG-I)-like receptor pathway (19). Viperin is also implicated as a

‡ These authors contributed equally.
* For correspondence: E. Neil G. Marsh, nmarsh@umich.edu.

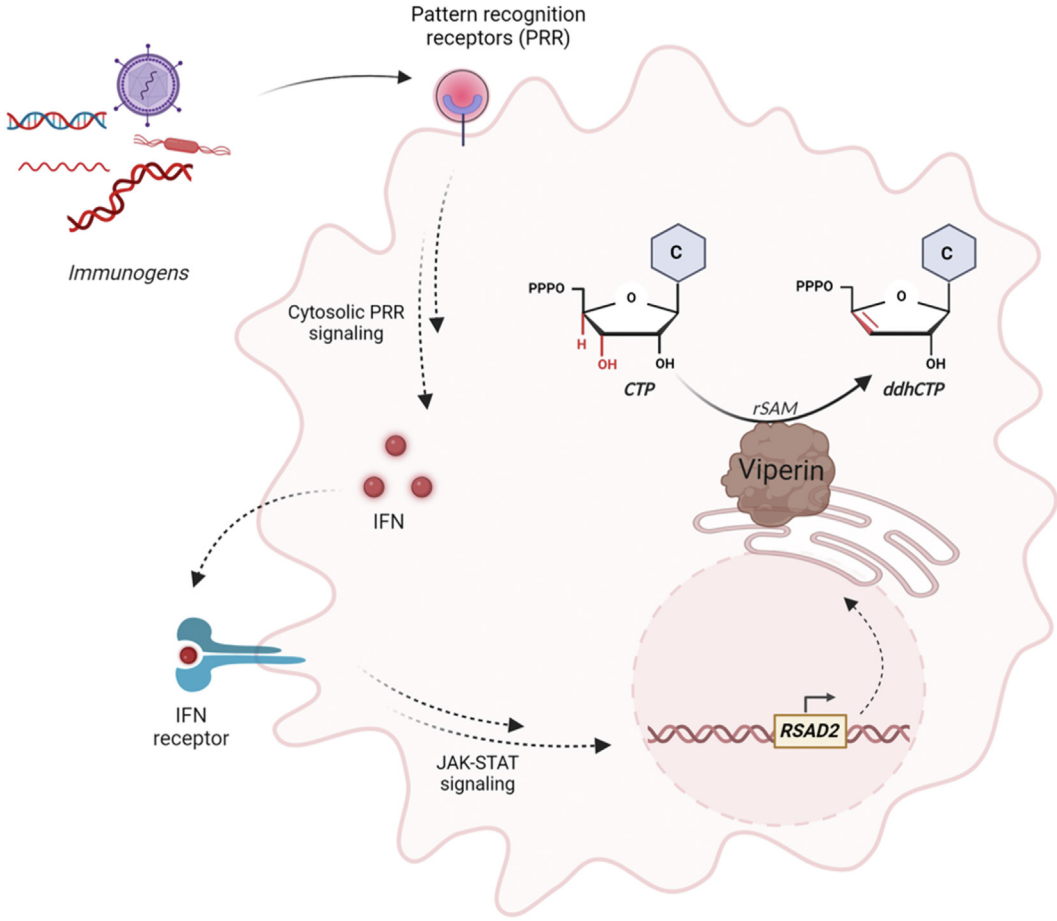

Figure 1. Induction of viperin expression. Viperin (*RSAD2*) is induced by a variety of immunogens such as external pathogens and internal cytokines. Viperin localizes to the endoplasmic reticulum (ER). It exerts its diverse roles in innate immunity by (*i*) synthesis of ddhCTP from CTP *via* radical SAM enzymology and (*ii*) interacts with key immune signaling proteins.

component of the TLR7/9 and cGAS-STING immune signaling pathways that ultimately result in type-I IFN upregulation. Although originally identified in the context of viral infection (20), *RSAD2* is increasingly recognized as a marker for autoimmune diseases and cancer (19): for example, *RSAD2* is highly upregulated in T cells from patients with SLE (8, 21) and in various cancers where its expression is correlated with poor survival rates (22).

The human mitochondrial genome comprises a 16,569 bp circular DNA that encodes two ribosomal RNAs, 22 transfer RNAs, and 13 essential subunits of the oxidative phosphorylation complexes (I, III, IV and V) (23–25). Although the mitochondrial genome is tiny, some 30% of the total RNA in metabolically active cells is mitochondrially encoded (1), pointing to the importance of mitochondrial transcription in cellular metabolism. Mt-encoded mRNAs are processed very differently from nuclear encoded genes. Whereas nuclear genes are transcribed as monocistronic transcripts that undergo splicing, polyadenylation, capping and export to the cytoplasm for translation, mitochondrial genes, in contrast, are transcribed from hundreds of copies of the circular genome as long, polycistronic RNAs (23–25). Only two primary transcripts are produced, referred to as the "heavy" and "light" strand transcripts; these are transcribed from opposing promoters situated close to the origin of replication and encompass almost the entire genome (Fig. 2*A*). The heavy strand transcript encodes the 2 mt-rRNAs, 14 tRNAs, and all but one (ND6) of the mitochondrially encoded OXPHOS proteins; the 'light' strand transcript encodes ND6, 8 tRNAs and non-coding regulatory RNAs (23). The transcripts are then cleaved by specific RNase enzymes to liberate individual mt-rRNAs, mt-tRNAs and mt-mRNAs; the mt-mRNAs are subsequently polyadenylated and then translated by mitochondrial ribosomes (23). Only 3 promoters direct mt-RNA production, and because of this, the regulation of transcription initiation is considered to contribute little to the levels of mt-encoded proteins (26). Rather, the secondary structures and stability of mt-mRNAs, which have half-lives much shorter than nuclear mRNAs, is an important factor affecting protein expression levels (26, 27).

The mt-RNA polymerase (POLRMT) is structurally most closely related to bacteriophage T3/T7 RNA polymerases (28) and many drugs developed as antiviral nucleotides have been found to have off-target toxicity against mitochondria (29). We therefore hypothesized that ddhCTP, which acts as a chain-terminating inhibitor of viral RNA-dependent RNA polymerases (17), might act similarly on POLRMT. Here we

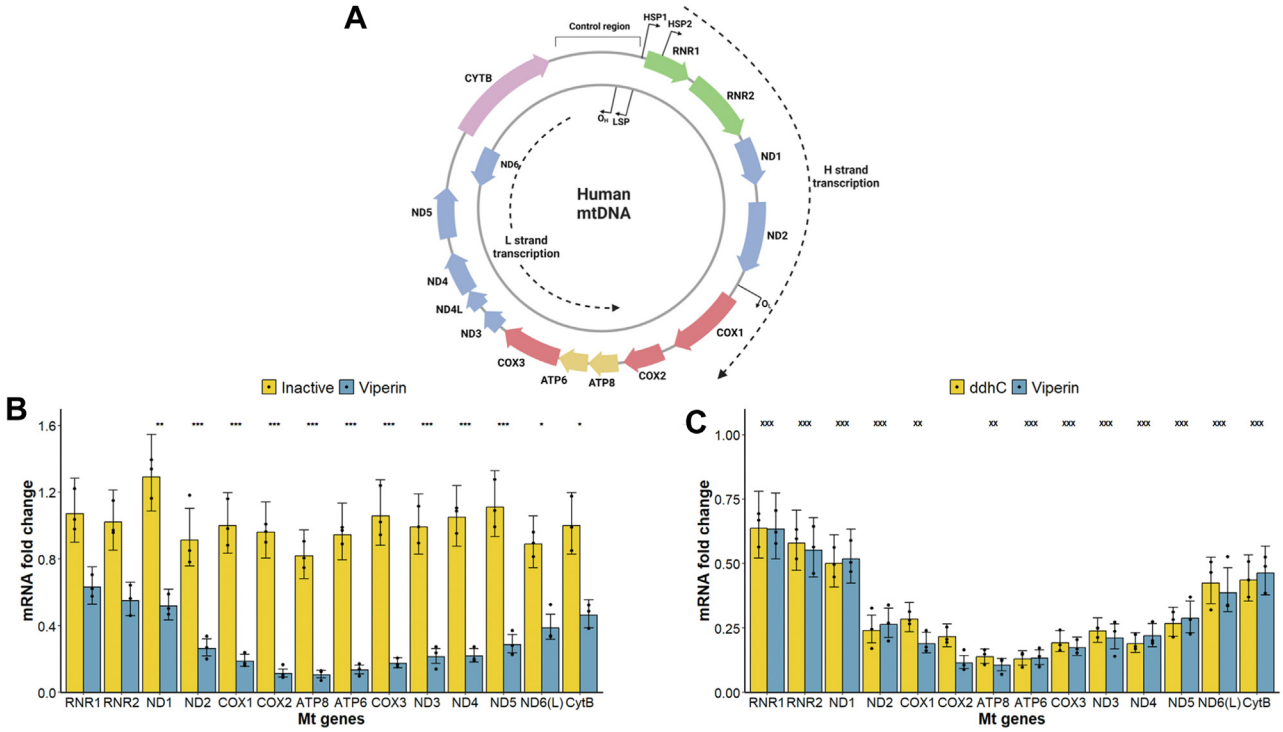

Figure 2. Viperin downregulates mitochondrial transcription by synthesizing ddhCTP. *A*, schematic of human mitochondrial genome showing the location of mt-rRNAs and mt-encoded OXPHOS genes. Positions of origins of replication (O_H and O_L), heavy strand promoters (HSP1, HSP2) and light strand promotors (LSP) are indicated; tRNAs are omitted for clarity. *B*, downregulation of mt-encoded genes in HEK293 T cells transfected with viperin requires active enzyme. RNA levels are determined by RT-qPCR 36 h post-transfection with wt-viperin or Δ3C-viperin (Inactive). Data were analyzed using a Bayesian model (see Methods for details); individual biological replicates from the RT-qPCR data are plotted as points ($2^{-\Delta\Delta Cq}$ for mRNA fold change and normalized to *NDUFAF3* gene from $n = 3$ experiments), and then the bar height and error bars show the posterior mean and 95% credible interval from the Bayesian analysis. Stars indicate the strength of evidence for a change of at least 1.5-fold between the Inactive and Viperin constructs, based on the Bayes factor (*: substantial evidence, BF > 3.2; **: strong evidence, BF > 10; ***: decisive evidence, BF > 100). *C*, comparison of ddhC supplementation and viperin transfection on mt-encoded gene expression. Cells were treated with the nucleoside analog, ddhC for 48 h. Data plotted as in panel b. In this case, significance markers show the strength of evidence for the difference between the ddhC and Viperin cases being less than 1.5-fold (x: substantial evidence, BF > 3.2; xx: strong evidence, BF > 10; xxx: decisive evidence, BF > 100).

demonstrate that viperin, through its production of ddhCTP, downregulates mt-gene expression, thereby providing a molecular-level mechanism for the downregulation of mitochondrial transcription that is associated with many human diseases.

Results

Viperin downregulates the expression of mt-genes

To investigate the effect of viperin expression on mitochondrial mRNA levels, we transiently expressed the protein in HEK293 T cells (Fig. S1). We designed PCR probes to report on both mt-rRNAs and each of the protein-encoding *OXPHOS* genes, and measured transcript levels 36 h after viperin transfection using RT-qPCR. Changes in mRNA levels of the individual mt-genes were normalized concerning both the nuclear-encoded housekeeping gene, *NDUFAF3* and to cells transfected with empty vector. Control experiments established that viperin expression did not alter the level of cellular mt-DNA (Fig. S2).

Although viperin expression decreased mitochondrial gene transcription (Fig. 2*B*), not all genes appeared similarly downregulated. Interestingly, we observed that the genes furthest from both the heavy and light strand transcriptional start sites, *e.g. ATP6* and *ATP8*, appear more strongly downregulated compared to those closer to either start site, *e.g. RNR1* and *CYTB*. Transfection with a catalytically inactive mutant Δ3C-viperin (Fig. S1), in which the three cysteine ligands coordinated to the essential [4Fe-4S] cluster were mutated to alanine, caused no significant change in mt-gene expression (Fig. 2*B*), suggesting that downregulation may result from ddhCTP synthesis. Co-expression of the ISG *CMPK2* (Fig. S1), the gene adjacent to *RSAD2*, that encodes a CDP kinase implicated in increasing CTP concentrations to provide the substrate for viperin did not further enhance mt-gene downregulation (Fig. S3).

To investigate whether ddhCTP is responsible for mt-gene downregulation, we cultured HEK293 T cells in the presence of 1 mM ddhC, which is taken up and phosphorylated to ddhCTP(17, 30). After exposure to ddhC for 48 h, the cells were harvested and mt-mRNA levels analyzed by RT-qPCR as described above. ddhC treatment showed a very similar pattern of mt-gene downregulation to that caused by viperin transfection (Fig. 2*C*). Additionally, varying the concentrations of ddhC revealed that 0.1 mM was not effective in downregulation of mt-genes (Fig. S4). These results suggest that the product of viperin, ddhCTP, is responsible for the downregulation of mt-encoded genes.

To further establish the link between ddhCTP synthesis by viperin and mt-gene downregulation, we examined whether viperin expression levels correlated with mt-gene downregulation as a function of time. HEK293 T cells were either transfected with viperin or supplemented with ddhC and harvested at 6 h intervals from 6 to 72 h after treatment. Relative mt-mRNA levels were then determined by RT-qPCR.

Viperin expression (Fig. 3*A*; Fig. S5) was maximal between 24 to 48 h post transfection. Again, genes furthest from transcriptional start sites appeared to be downregulated the most, with expression levels recovering as the concentration of viperin decreased after 48 h (Fig. 3*A*; Fig. S6). mRNA levels were strongly anti-correlated with viperin protein levels (determined by immunoblotting) with R^2 ranging from 0.65 to 0.84 for genes that were most heavily downregulated such as *ATP8*. A similar pattern of downregulation was observed in cells grown in the presence of ddhC (Fig. 3*B*; Fig. S6); in this case the lag in downregulation presumably reflects the kinetics of ddhC uptake and phosphorylation. These experiments provide further evidence that viperin-induced downregulation of mt-gene transcription is due to the production of ddhCTP and that it is both transient and reversible.

ddhCTP downregulates mt-gene expression through chain-termination inhibition of POLRMT

We hypothesized that the pattern of mt-gene downregulation may be due to ddhCTP acting as a chain-terminating inhibitor of transcription when misincorporated by POLRMT, similarly to how it functions as an antiviral ribonucleotide when misincorporated by viral RNA-dependent RNA polymerases (17, 30). Mitochondrial genes are transcribed as long polycistronic RNAs that span almost the entire genome. The cumulative probability of termination due to misincorporation of ddhC increases with distance from the transcription start site, therefore genes furthest from the promoter will appear more downregulated. Note that because the "heavy" strand and "light" strand transcripts almost entirely overlap, and reverse transcription was performed using random priming, the qPCR reporter probes report on the *sum* of both transcripts as a function of position. Thus, the apparent increase in mRNA levels of genes situated towards the end of the "heavy" strand, *e.g. CYTB*, is artifactual—most of the mRNA detected by RT-qPCR for these genes will come from the non-coding "light" strand transcripts.

To further test whether chain termination could account for the pattern of mt-gene downregulation, we compared the effects on mt-gene transcription due to 3′-deoxycytidine (3′-dC), 2′,3′-dideoxycytidine (ddC) and IMT1 which is a specific allosteric inhibitor of POLRMT (31). 3′-dC, lacking a 3′-hydroxyl group, was expected to be a good chain-terminating inhibitor, whereas ddC was predicted to be a weak chain-terminating inhibitor because the 2′-hydroxyl group is an important recognition element for RNA polymerases. The RT-qPCR data for HEK293 T cells treated with cytidine, 3′-dC, ddC, ddhC, or IMT1 (Fig. 4*A*; Fig. S7) supports our hypothesis. ddC weakly inhibited transcription, whereas 3′-dC strongly downregulates transcription in a pattern very similar to ddhC, indicating that it may also act as a chain-terminating inhibitor. IMT1, by contrast, strongly suppressed transcription of all the mt-genes by similar amounts, consistent with it being a potent

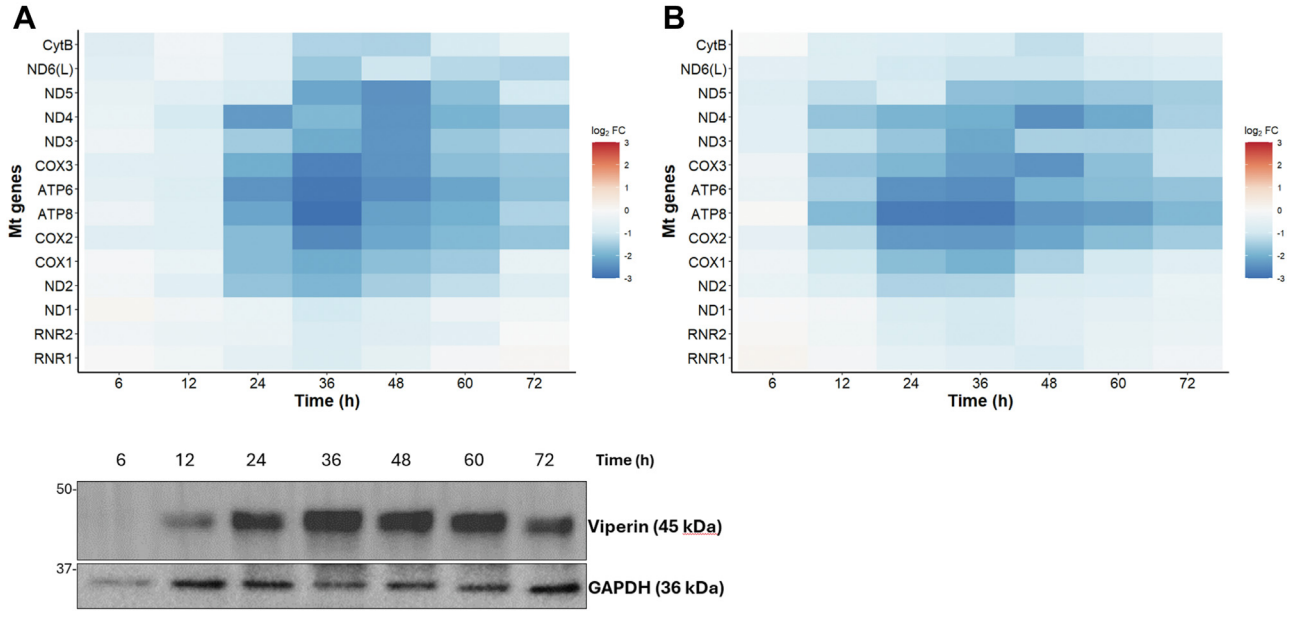

Figure 3. Time dependent downregulation of mt-genes with viperin transfection and ddhC treated HEK293 T cells. *A*, heatmap representing downregulation of mt-genes with viperin transfection from RT-qPCR analysis. Cells were transfected with viperin and harvested after the indicated time points. Quantitative immunoblot represents the levels of viperin in the cell from 6 to 72 h. *B*, heatmap representing downregulation of mt-genes with ddhC supplementation from RT-qPCR analysis. Cells were supplemented with 1 mM ddhC and harvested after the indicated time points. Mt-genes are listed in the y-axis with increasing distance from the mitochondrial origin of replication. mRNA fold change ($2^{-\Delta\Delta Cq}$) was measured by RT-qPCR analysis and normalized to *NDUFAF3* gene from $n = 3$ experiments.

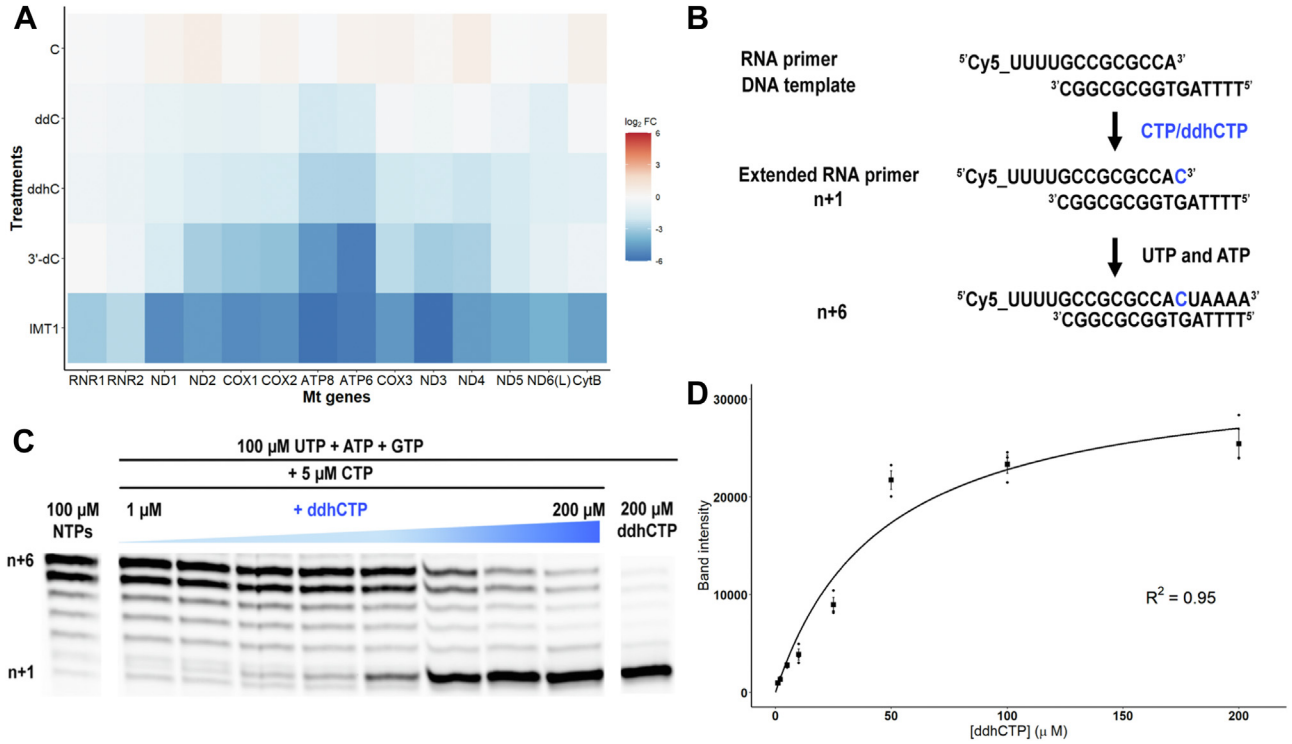

Figure 4. Downregulation of mt-genes by chain-terminating CTP analogs occurs through misincorporation by POLRMT. *A*, heatmap showing the effect of cytidine (C, control), 2′,3′-dideoxycytidine (ddC), ddhC, 3′-deoxycytidine (3′-dC) and the allosteric inhibitor IMT1 on mt-encoded gene expression. Mt-genes are listed in the x-axis with increasing distance from the mitochondrial origin of replication. mRNA fold change ($2^{-\Delta\Delta Cq}$) was measured by RT-qPCR analysis and normalized to *NDUFAF3* gene from $n = 2$ experiments. *B*, schematic of *in vitro* RNA-primer extension assay. *C*, representative gel showing misincorporation of ddhCTP by POLRMT with increasing ddhCTP concentrations. *D*, plot of band intensity (*I*, arbitrary units) for ddhCTP incorporation (n + 1 band) as a function of [ddhCTP]. The data are fitted to the equation $I = I_{max} * \left(\frac{[ddhCTP]}{D_{app}+[ddhCTP]}\right)$ where I_{max} is the maximum intensity for the ddhCTP band and D_{app} is the apparent discrimination constant at fixed [CTP]. Data represents an average of $n = 3$ experiments; fitting parameters are given in Table S7.

allosteric inhibitor of POLRMT(31). The treatment of 3′-dC and IMT1 on Huh-7 showed a similar pattern of downregulation of mt-genes as in HEK293 T (Fig. S11*A*).

ddhCTP is efficiently misincorporated by POLRMT

To further support our hypothesis we examined whether POLRMT misincorporates ddhCTP by conducting transcription read-through assays (17) with purified, recombinant human POLRMT (32) (Fig. S12*A*). These experiments used a synthetic oligonucleotide template, and a fluorescently labelled RNA primer designed so that a unique 'G' in the template strand directs the addition of a 'C' to the primer at the +1 position. Incorporation of CTP allows read-through, resulting in extension of the primer by 6 nucleotides, whereas misincorporation of ddhCTP terminate extensions with addition of only ddhC (Fig. 4*B*).

As shown in Fig. 4*C*, ddhCTP is incorporated into RNA by POLRMT and with increasing concentration effectively competes with CTP. From these data the discrimination factor, $D = [k_{pol}/K_d]^{CTP}/[k_{pol}/K_d]^{ddhCTP}$ of POLRMT for CTP over ddhCTP was calculated to be ∼ 10; a similar was obtained when [ddhCTP] was held constant and [CTP] varied (Fig. S13, Table S7). This value is surprisingly low: for context, the discrimination factors for CTP over ddhCTP measured previously using similar methodology for West Nile virus and Dengue virus RNA-dependent RNA polymerases were 59 and 135 respectively (17). It is also lower than the discrimination factors previously measured for the misincorporation of other antiviral nucleotides such as C2′-methyl-ATP by POLRMT (29). Similar experiments with 3′-dCTP revealed a comparable discrimination factor of ∼ 7 consistent with our hypothesis that these molecules are similar in their mechanism of misincorporation by POLRMT (Fig. S14, Table S8). However, while this experiment demonstrates the ability of POLRMT to incorporate ddhCTP, as we discussed below, in cells the misincorporation of ddhCTP into mt-RNA must occur much less frequently than the low discrimination factor might suggest.

ddhC downregulates mt-transcription across multiple cell types

To assess the generality of ddhCTP to modulate mitochondrial transcription, we examined the effect of ddhC on a panel of 14 immortalized human cell lines derived from a range of tissues. These included B and T lymphoblasts, monocytes and promyeloblast cell lines derived from the immune system, breast, liver, bone and skin cancer cell lines (Table S4). A heat map summarizing the expression data for 15 cell lines (including HEK293 T) we examined is shown in Figure 5*A*. Although some cell lines appear more sensitive to ddhC than others, in most cell lines we observed a similar 'U'-shaped pattern of mt-gene downregulation (Figs. 5*A* and S8)

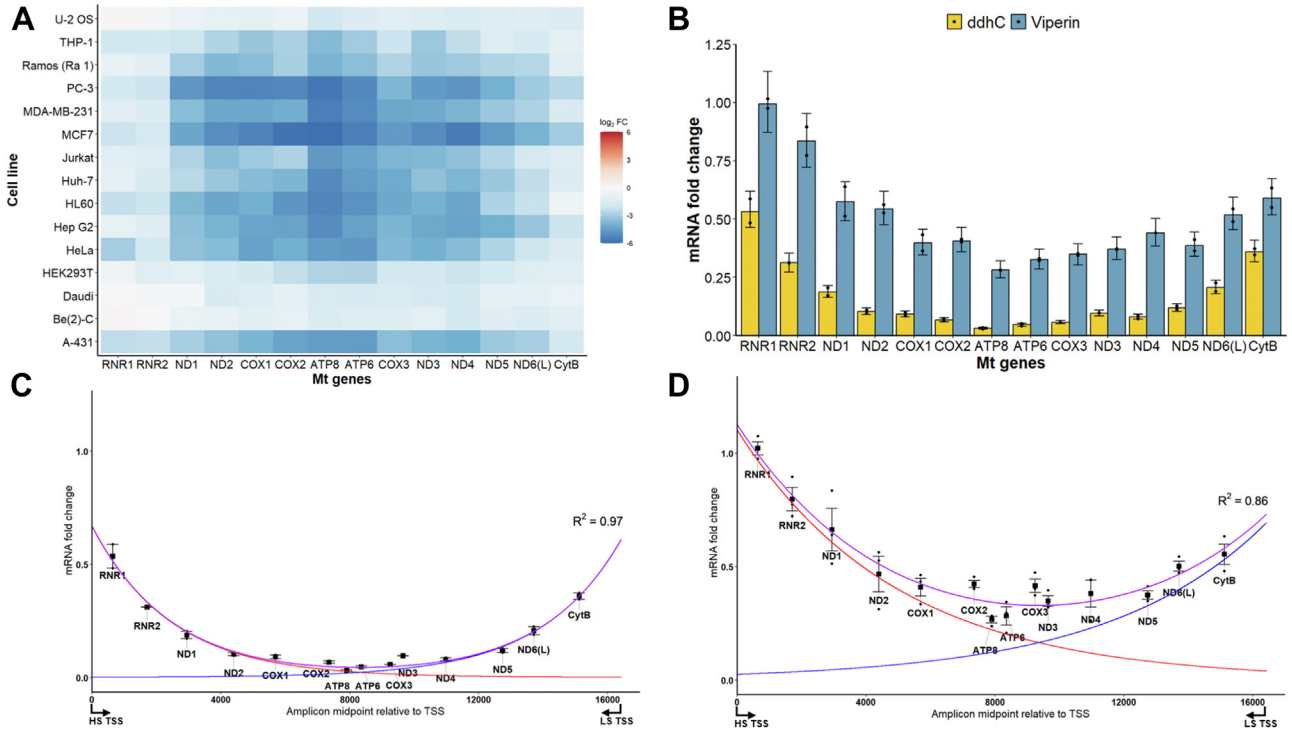

Figure 5. ddhC induces mt-encoded gene downregulation in multiple cell lines; the pattern of downregulation fits a model of random transcriptional chain termination. *A*, heatmap showing ddhC-induced downregulation of mt-encoded genes across 15 human cell lines. Cells harvested 36 to 48 h after addition of ddhC. Mt-genes are listed in the x-axis with increasing distance from the mitochondrial origin of replication. mRNA fold change ($2^{-\Delta\Delta Cq}$) was measured by RT-qPCR analysis and normalized to *NDUFAF3* gene from $n = 2$ experiments. *B*, representative data from Huh-7 cells either transfected with viperin (*blue*) or supplemented with ddhC (*gold*). Data were analyzed using a Bayesian model (see Methods for details); individual biological replicates from the RT-qPCR data are plotted as points ($2^{-\Delta\Delta Cq}$ for mRNA fold change and normalized to *NDUFAF3* gene from $n = 2$ experiments), and then the bar height and error bars show the posterior mean and 95% credible interval from the Bayesian analysis. *C* and *D*, data from (*B*) plotted as a function of the distance from the heavy and light strand transcription start site (HS TSS, LS TSS) and fitted to Equation 1 (*purple* line), which describes a model for random mt-RNA chain termination by ddhCTP. The implied abundances of heavy (*red* line) and light (*blue* line) transcripts are indicated on the plot and obtained by deconvoluting the data into the component exponential decay functions in Equation 1. *C*, Huh-7 cells supplemented with ddhC. *D*, Huh-7 cells transfected with viperin.

suggesting that ddhCTP-induced downregulation of mt-genes is a general phenomenon.

To further interpret the data, we consider a simple quantitative model that describes the reduction in mRNA levels due to chain-termination. Assuming the probability of POLRMT of misincorporating ddhCTP at each 'C' it transcribes is similar, the abundance of the transcript should decay exponentially as a function of the distance from the transcription start sites. This situation can be modeled by a simple 2-exponential function represented by Equation 1, which accounts for transcription from both 'heavy' and 'light' strand transcription start sites.

$$f_n = F_h e^{-P_{mis} n} + F_l e^{-P_{mis}(\Delta - n)} \qquad \text{(Eq. 1)}$$

f_n represents the relative amplitude of the qPCR signal at position n on the chromosome relative to the first heavy strand start site; Δ = 16,413 is the separation in nucleotides between the heavy- and light-strand transcription start sites; and the decay constant P_{mis} represents the probability of misincorporating ddhCTP at each nucleotide transcribed. The pre-exponential factors, F_h and F_l, describe what fraction of the change in the heavy and light strand transcript levels, respectively, can be ascribed to chain termination. F_h and F_l are expected to be > 0.5 if chain termination contributes significantly to downregulation.

The RT-qPCR data from all the cell lines represented in Figure 5*A*, and for Huh-7 cells (Fig. 5*B*) were fitted to Equation 1 (Fig. 5, *C* and *D* and Figures S9–S11*B*; fitting parameters given in Tables S9–S11). For viperin-transfected Huh-7 cells (Fig. 5*D*), Equation 1 adequately accounts for most of the variation in transcript levels, with F_h = 1.1, F_l = 0.7, R^2 = 0.84. For Huh-7 cells treated with ddhC (Fig. 5*C*), Equation 1 also fits the data well, R^2 = 0.97, but in this case, there appears to be a termination-independent component to the decrease in mt-RNA levels which shows up in smaller values of F_h and F_l, which are 0.7 and 0.6 respectively. In majority of the cell lines we examined, fitting the data to Equation 1 could account for $>$ 50% of the decrease in mt-RNA transcript levels observed in response to ddhC treatment (see Table S11). Although in most cell lines ddhC appears to suppress mt-RNA levels in a termination-independent manner to some degree. The frequency of ddhCTP misincorporation can be estimated from P_{mis} which varied between $\sim$ 0.0002 and $\sim$ 0.0005 in our experiments. For Huh-7 cells either treated with ddhC or transfected with viperin (Fig. 5, *C* and *D*) P_{mis} values are $\sim$ 0.0004 and $\sim$ 0.0002 respectively (Table S9). These values indicate that

under these conditions ddhCTP misincorporation occurs with an approximate frequency of once for every 750 to 1500 cytidine bases transcribed.

Discussion

The dysregulation of mitochondrial metabolism is an important feature of many inflammatory diseases in which impaired oxidative phosphorylation leads to the production of ROS and an inflammatory cascade (1, 4–6). Although it was shown over 30 years ago that IFN stimulation causes downregulation of mt-encoded OXPHOS genes with a concomitant suppression of cellular respiration and ATP synthesis (11), the mechanism by which this occurs has remained unknown.

Noting that *RSAD2* is one of the most highly upregulated ISGs (33), we propose that synthesis of ddhCTP by viperin results in premature chain-termination of mt-RNA transcripts when ddhCTP is misincorporated by POLRMT (Fig. 6). In support of this mechanism, we have demonstrated that either viperin transfection or supplementing cells with ddhC results in the position-dependent pattern of mt-gene downregulation. Significantly, the observed pattern of gene downregulation fits well to a model in which chain termination progressively lowers transcript levels, whereas it is not explained by simple noncovalent inhibition of POLRMT. We have also shown that ddhCTP is readily misincorporated by POLRMT *in vitro*, which is consistent with previous studies showing that many antiviral drugs targeted to viral RNA-dependent RNA polymerases are cytotoxic due to their interaction with POLRMT (29).

The regulation of mitochondrial gene expression differs significantly from the far more complex nuclear genome (24, 25). mt-mRNA levels appear to be regulated primarily by nuclear-encoded RNA-binding proteins such as LRPPRC (27) that modulate mt-mRNA stability and hence the rate at which it is degraded (26, 27). In this context, the downregulation of mt-encoded genes by ddhCTP, which results in both dose-dependent and position-dependent attenuation of mRNA transcript levels, represents an additional and efficient mechanism by which cells may control mitochondrial metabolism.

Chain-terminating nucleotides have generally been considered only as inhibitors of viral replication. Our studies point to chain termination as a mechanism for controlling gene expression, a function for ddhCTP that has not been previously recognized. Another recent study showed that production of ddhCTP by viperin induces ribosome collisions in cells (34), which, in turn, triggers the integrated stress response (35) and thereby globally downregulates protein synthesis. Although the mechanism by which ddhCTP causes ribosome collisions remains unknown (34), these results support the idea that ddhCTP plays an important, multifunctional role in the innate immune response.

Our measurements on purified POLRMT show it discriminates between ddhCTP and CTP rather poorly, favoring CTP by a factor of only ~ 10. Previous studies have measured ratios of ddhCTP to CTP ranging 1:7 – 1:10 in cells either transfected with viperin or cultured with ddhC(17), which *in vivo* would translate to the misincorporation of ddhCTP once every 70 to 100 cytidine bases transcribed. However, the frequency of misincorporation *in vivo*, estimated from fitting gene expression data to Equation 1, is significantly lower, only ~ 1 in 750 to 1500 cytidine bases transcribed. The reasons for this discrepancy are unclear but include the possibility that nucleotide ratio may be much more heavily skewed against ddhCTP in the mitochondria than in the cytosol and/or that POLRMT may exhibit higher selectivity when transcribing a

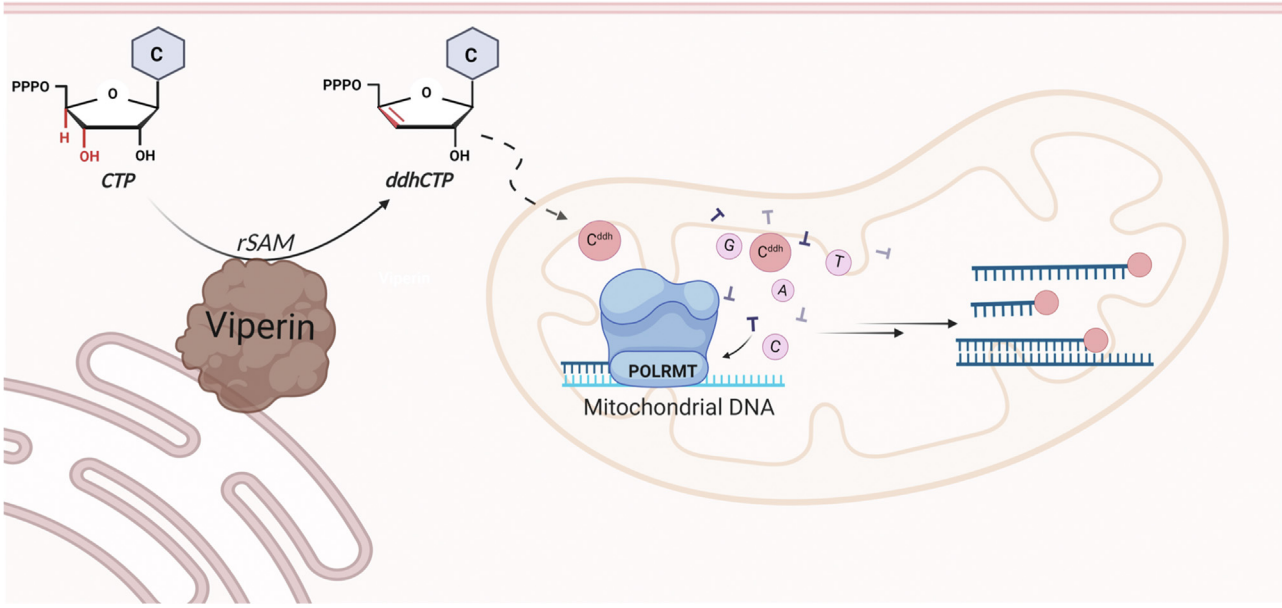

Figure 6. Proposed mechanism for viperin-mediated downregulation of mitochondrial transcription. ddhCTP is synthesized in the cytoplasm by ER-bound viperin and imported into the mitochondrion. ddhCTP is misincorporated by POLRMT during bidirectional, mitochondrial transcription resulting in premature termination of mt-RNA polycistronic transcripts.

physiological transcript in the presence of mt-transcription and elongation factors (24, 29, 36). Furthermore, given the rapid turnover of mt-mRNA(26), RT-qPCR measurements of transcript levels may underestimate the rate of ddhCTP misincorporation. This would occur if prematurely terminated transcripts were more rapidly degraded and therefore undersampled by RT-qPCR.

An intriguing question is whether the downregulation of mt-OXPHOS genes by viperin is purely pathological or serves some broader physiological purpose. Both mitochondria and viperin are of ancient origin (16, 37) and are likely to have co-evolved in cells. Therefore, if misincorporation of ddhCTP was disadvantageous, POLRMT variants would likely have evolved that better discriminate against ddhCTP, as some viral RNA-dependent RNA polymerases appear to have done (17). We suggest, instead, that this mechanism of regulating mt-encoded gene expression may play a physiological role in regulating oxidative phosphorylation. In support of this idea, an increasing number of studies have demonstrated connections between viperin and mitochondrial metabolism (19): for example, viperin can be translocated into mitochondria where it inhibits fatty acid β-oxidation (38, 39) and may play a role in controlling thermogenesis in adipose tissue (40).

Our studies used transfected proteins in immortalized cell lines, but there is good reason to believe that this mechanism of transcriptional regulation is relevant to the altered cellular physiology observed in many cancers (41) and inflammatory diseases (19). It is well established that viperin is highly upregulated in various immune cells upon stimulation with interferons (13, 42). Notably, in $CD4^+$ and $CD8^+$ T cells derived from patients with SLE, viperin was found to be highly upregulated and the mt-OXPHOS genes correspondingly moderately downregulated (8, 9). *RSAD2* is also reported to be upregulated in various cancers where its expression has been found to be under control of the PI3K/AKT/mTOR/HIF-1α signaling pathway (22). This signaling pathway is activated in many cancers and underpins the upregulation of glycolysis under normoxic conditions known as the Warburg effect (43). Although the significance of ddhCTP-induced mitochondrial dysfunction in the Warburg effect is unclear, it is notable that *RSAD2* contains a hypoxia-responsive–binding element within the 5′-promoter region and viperin expression is upregulated in response to hypoxia (22). This finding hints that viperin, which like all radical SAM enzymes, is very oxygen sensitive (14), may be part of an ancient response to hypoxia and mitochondrial metabolism.

In conclusion, our studies demonstrate a molecular-level mechanism for the IFN-induced downregulation of mt-OXPHOS genes that contributes to mitochondrial dysregulation observed in SLE patients (7, 8), and other diseases characterized by chronic inflammation. The mechanism involves the synthesis of ddhCTP by viperin, which then acts as a chain-terminating inhibitor of RNA transcription by POLRMT. ddhCTP-induced transcription termination provides a simple, efficient and tunable means of modulating mt-OXPHOS gene expression. Viperin is one of the only eight radical SAM enzymes in the human genome (15) and the radical-mediated dehydration of CTP to ddhCTP is, mechanistically, a unique enzyme reaction. Therefore, drugs targeted to viperin may be a promising route to explore in developing therapeutic approaches to inflammatory diseases.

Experimental procedures

Cell culture

All cell lines (Table S1) were cultured in 10 cm dishes in appropriate complete medium (Supporting Information S1–S2) at 37 °C under a 5% CO_2 and humidified atmosphere. Plasmids (20 μg, Table S4) were transfected in HEK293 T and Huh-7 cells at 50 to 60% confluency using PEI MAX (Kyfora Bio; 24,765–100). CMPK2 and viperin were co-transfected (10 μg per plasmid) in HEK293 T cells. Cells were harvested at the indicated time points for immunoblotting and RT-qPCR analysis. For ddhC treatment, cells were supplemented with ddhC (1 mM) in culture media and harvested within 36 to 48 h for RT-qPCR analysis. Additionally, ddhC was supplemented at 0.1 mM and 0.5 mM in HEK293 T cells and harvested after 48 h. Nucleoside analogs (1 mM) and IMT1 (POLRMT inhibitor, 10 μM) were supplemented in culture media and harvested after 48 h.

SDS-PAGE and immunoblotting

10^6–10^7 cells (HEK293 T and Huh-7) were harvested from 10 cm plates, washed with PBS and gently resuspended in 450 to 500 μl of lysis buffer (50 mM Tris-HCl pH 7.5, 500 mM NaCl, 1% Tween-20, supplemented with 1X protease and phosphatase inhibitor cocktail and 0.1 mM PMSF). After incubation on ice for 15 min, cells were lysed by sonication and lysates cleared by centrifugation in a microcentrifuge at 18,000 x g for 10 min at 4 °C. The BCA assay (Pierce BCA protein assay kit; 23,227, Thermo Fisher Scientific) was used to determine protein concentrations. 20 to 30 μg of total protein per sample was mixed with 4X loading dye (Table S3) supplemented with 10% βME, denatured at 95 °C for 10 min and separated by SDS-PAGE. After SDS-PAGE, proteins were transferred onto methanol-activated PVDF membranes (Table S3) using wet-transfer at 400 mA at 4 °C for 1 h in pre-chilled transfer buffer (25 mM Tris-HCl pH 8.3, 192 mM glycine, 20% (v/v) methanol). The membranes were blocked with 5% non-fat dried milk in TBS-T (tris-buffered saline plus 0.05% Tween-20) for 1 h at room temperature. Incubation with primary antibodies (Table S3) was performed at a dilution of 1:1000 for all the antibodies, except for anti-GAPDH, which was diluted 1:5000 (or 9000), and at 4 °C overnight. Blots were developed by washing with TBS-T (3-times), probing with 1:2500 diluted HRP-conjugated secondary antibodies (Table S6), washing again (3-times) and imaging on a Chem-iDoc MP imaging system (Bio-Rad) using chemiluminescent substrate (Supporting Information S6).

RT-qPCR analysis

Total RNA was extracted from ∼10^5–10^7 cells, lysed in TRI reagent (R2050-1-50, Zymo Research) and purified using

Direct-zol RNA Miniprep Plus kit (R2072, Zymo Research). The eluted RNA was subjected to DNase digestion for 1.5 h at 37 °C using Baseline-Zero DNase (DB0715 K, Biosearch Technologies) and was further cleaned using RNA Clean & Concentrator-5 (R1016, Zymo Research). The purified RNA (0.5–1 μg) was reverse transcribed using the ProtoScript II Reverse Transcriptase (M0368 L, NEB) using Random Primer Mix (S1330S, NEB) according to the manufacturer's protocol. RT-qPCR was performed using the iTaq Universal SYBR Green Supermix (1,725,121, Bio-Rad). 10 μl qPCR reactions with 2 to 20 ng of cDNA (concentration was measured assuming full conversion from purified RNA) and gene-specific primers at 600 nM final concentration (Table S6) were pipetted in 384 well plate (Axygen 384-well Skirted PCR Microplates, 14,222,310, Thermo Fisher Scientific). The data were recorded on the CFX Opus 384 Real-Time PCR system (Bio-Rad) and analyzed using Bio-Rad CFX Maestro software 2.0 (v. 5.0.021.0616). Recorded Cq values of experimental samples were first normalized against control (empty vector) treatments harvested at same time and then normalized to the recorded Cq of human *NDUFAF3* as our control gene. Data were plotted as $2^{-\Delta\Delta Cq}$ to reflect mRNA fold change (relative expression). The qPCR cycle steps were as follows: (*i*) 95 °C, 2 min; (*ii*) 95 °C, 10 s; (*iii*) 60 °C, 30 s; (*iv*) 39 cycles of (*ii*)–(*iii*); (*v*) 65 °C–95 °C, 5 s, +0.5 °C/cycle.

Expression and purification of recombinant proteins

Expression vectors for UCK2, CMPK1 and NDK were kindly provided by Dr Tyler L. Gove (Albert Einstein College of Medicine). A gene encoding human mitochondrial RNA polymerase (POLRMT) (44) (residues 44–1230) with an N-terminal 6xHis tag was synthesized commercially (Genscript) and cloned into pET-28a (+) vector. All constructs were expressed in *E. coli* BL21(DE3) (C2527H, NEB).

UCK2, CMPK1 and NDK were expressed and purified following the previous literature with a slight modification (45). Protein expression was induced at OD_{600} = 0.7 to 0.9 with 0.5 mM isopropyl β- D-thiogalactopyranoside (IPTG). Cell pellets were resuspended in lysis buffer (50 mM HEPES, pH 7.5, 300 mM KCl, 10% glycerol (v/v), 5 mM βME), and lysed by sonication at 4 °C. The lysate was cleared by centrifugation at 12,000 x g for 1 h at 4 °C. The supernatants were loaded onto a His-trap HP column (17,524,802, Cytiva) equilibrated with lysis buffer. The column was washed with lysis buffer—12 column volumes, and additional 5 column volumes with lysis buffer containing 40 mM imidazole. The proteins were eluted with elution buffer (50 mM HEPES, pH 7.5, 300 mM KCl, 10% glycerol (v/v), 5 mM βME, 500 mM imidazole). Protein-containing fractions were concentrated and further purified by size-exclusion chromatography with the column (Superdex 200) equilibrated with buffer (50 mM HEPES pH 7.5, 300 mM KCl, 5% glycerol (v/v), 5 mM DTT). Purified protein fractions were pooled, and concentrated (∼200 μM), flash frozen, and stored in −80 °C. Proteins were greater than 95% pure as analyzed by SDS-PAGE electrophoresis.

POLRMT was purified based on a previously described protocol (46) with minor modifications. Cells were grown in 2xYT media after inoculation with overnight culture (grown in LB). Protein expression was induced at OD_{600} = 0.7 to 0.9 with 0.2 mM IPTG after cold shock at 4 °C for 20 min. Cells were harvested by centrifugation after 18 h shaking at 16 °C. Cell pellets were resuspended in lysis buffer (50 mM Tris, pH 8.0, 400 mM NaCl, 10 mM imidazole, 5% glycerol (v/v), 5 mM βME, 0.1% Tween 20 (v/v)) supplemented with PIC cocktail (11,873,580,001, Millipore Sigma) and sonicated. Cell debris was removed by centrifugation at 12000 x g for 1 h at 4 °C, and the supernatant loaded onto a His-trap HP column. The column was washed with 12 column volumes of lysis buffer and 5 column volumes of lysis buffer containing 40 mM imidazole. The protein was eluted with elution buffer (50 mM Tris pH 8, 300 mM NaCl, 200 mM imidazole, 5% glycerol (v/v), 5 mM βME, 0.1% tween 20 (v/v)). Samples were diluted and a second round of His-trap affinity purification was performed to remove persistent contaminating proteins. The fractions containing POLRMT were confirmed by SDS-PAGE, buffer exchanged in storage buffer (50 mM Tris pH 8, 5% glycerol, 150 mM NaCl, 0.1% Tween 20, 1 mM DTT), and then concentrated to ∼4 μM and stored at −80 °C.

Phosphorylation of 3′-deoxy-3′,4′-didehydro-cytidine (ddhC) and 3′-deoxycytidine (3′-dC)

Stock solutions of ddhC and 3′-dC (50 mM) were made in 500 mM HEPES, pH 7.5. 1 ml phosphorylation reactions were carried out in a reaction buffer (20 mM HEPES, pH 7.5, 100 mM KCl, 10 mM $MgCl_2$ and 10 mM βME). In the reaction mixture, 10 μM of each of the kinases—UCK2, CMPK1, and NDK were added along with 100 μM ATP, 3 mM phosphoenolpyruvate (SS-9762, Combi-Blocks) and 10 units of pyruvate kinase (ICN15199901, Thermo Fisher Scientific). The reactions were initiated by addition of ddhC or 3′dC, 1 mM final concentration. After 2 h incubation at room temperature, reactions were quenched with one drop of concentrated HCl and titrated to pH 7.5 using 1 M Tris-Cl (pH 7.5).

Purification of ddhCTP and 3′-dCTP

Phosphorylated nucleotides were diluted to 10 ml using buffer A (20 mM ammonium bicarbonate, pH 9.0; 09,830, Millipore Sigma) were loaded onto a HiTrap Q HP 5 ml anion exchange column (Cytiva) using AKTA FPLC Purifier at a flow rate of 2 ml/min. The column was washed with 5 column volumes of buffer A and phosphorylated products were eluted with a linear gradient of buffer B (500 mM ammonium bicarbonate, pH 9.0) at a flow rate of 4 ml/min over 30 column volumes. ddhCTP and 3′-dCTP both eluted at ∼36% of buffer B and was flash frozen and lyophilized.

POLRMT primer extension assays with ddhCTP and 3′-dCTP

Primer extension assays were performed based on previously described protocols. As shown in Figure 4*A*, a 15 nt

DNA template and a 13 nt 5′-Cy5-labelled RNA primer designed with a 4 nt 5′-overhang (10 μM each) were annealed in 10 mM Tris (pH 8.0) and 1 mM EDTA by heating the mixture at 90 °C for 1 min and then slowly cooled (5 °C/min) to 10 °C[4]. The scaffold (500 nM) was mixed with 1 μM POLRMT in a reaction buffer (100 mM Tris, pH 8.0, 5 mM $MgCl_2$, 50 mM DTT, 0.25% Tween 20) and 100 μM of each of ATP, UTP and GTP were added. Various concentrations of CTP, ddhCTP or 3′-dCTP were added to the reactions. Reaction mixtures were incubated at 30 °C for 10 min before quenching with EDTA, final concentration 50 mM.

Samples were diluted with an equal volume of loading buffer, 20 μl, (100% formamide, 500 mM EDTA, 10% SDS) and heated at 90 °C for 5 min 8 μl of each sample was loaded on a 23% polyacrylamide gel containing 1xTBE (BP13334, Thermo Fisher Scientific) as running buffer—89 mM Tris, 89 mM borate, 2 mM EDTA and 6 M urea. Electrophoresis was performed at 30 W for 2 h. Gels were imaged using the Amersham Typhoon NIR Plus (Cytiva) and fluorescence intensity was quantified by ImageJ (v.1.54) software and normalized against the n + 1 band for each experiment.(32)

Data analysis and statistics

All curve fitting and data plotting were performed on RStudio (v. 2024.04.2 Build 764) and represented as mean ± sd of multiple experiments as annotated in figure legends and experimental procedures. All illustrations were generated using BioRender. Uncropped immunoblots, SDS-PAGE images and raw data are provided in Supporting Information.

RT-qPCR data were analyzed using a Bayesian framework to provide both credible intervals and rigorous testing, aiming to either accept or reject a null hypothesis, as appropriate. The analyzed values consist of the average of technical replicates across an experiment, analyzed using a Bayesian framework as implemented in the R package, brms (47). A Student-t distributed model was used with default priors, featuring one intercept term for each replicate pair and an additional term Viperin or ddhC treatment, as appropriate. A single unified intercept term was used for the variance and degrees of freedom parameters for each of the variance and degrees of freedom parameters. All models converged based on the visual inspection of sampling traces and the Rhat criterion. Figures display 95% credible intervals from the posterior distribution. Additionally, we assigned significance based on the Bayes Factor of the hypothesis that the fold change for the indicated treatment was either greater than 1.5-fold (Fig. 2*B*) or less than 1.5-fold (Fig. 2*C*). The Bayes Factors were interpreted according to the scale of Kass and Raftery (48), as stated in the figure caption. It should be noted that the Bayesian model is especially useful for the analysis shown in Figure 2*C* as it allows for the direct quantitation of evidence for the null hypothesis of no difference between the Viperin and ddhC treatments.

Data availability

The primary rt-PCR data used to analyze mitochondrially encoded gene expression levels are available from the corresponding author upon request.

Supporting information—This article contains supporting information.

Acknowledgments—We thank the members of the Marsh group for helpful discussions.

Author contributions—SJ. L., R. H., S. M., P. R., and M. J. investigation; R. H., L. F., and E. N. G. M. supervision; L. F., E. N. G. M., S. M., and P. R. writing–review & editing, L. F. methodology; L. F. and E. N. G. M. funding acquisition; L. F. and P. R. formal analysis. E. N. G. M., S. M., and P. R. writing–original draft; E. N. G. M. project administration; E. N. G. M. and S. M. conceptualization.

Funding and additional information—This study was supported by NIH grants GM093088 and GM153307 to E.N.G.M., and GM128637 to L.F.

Conflicts of interest—The authors declare that they have no conflicts of interest with the contents of this article.

Abbreviations—The abbreviations used are: ddCTP, 3′-deoxy-3′,4′-didehydrocytidine triphosphate; mt-genes, mitochondrially encoded genes; OXPHOS, oxidative phosphorylation; POLRMT, mitochondrial RNA polymerase; RA, rheumatoid arthritis; SLE, systemic lupus erythematosus.

References

1. Harrington, J. S., Ryter, S. W., Plataki, M., Price, D. R., and Choi, A. M. K. (2023) Mitochondria in health, disease, and aging. *Physiol. Rev.* **103**, 2349–2422
2. Dhir, A., Dhir, S., Borowski, L. S., Jimenez, L., Teitell, M., Rötig, A., *et al.* (2018) Mitochondrial double-stranded RNA triggers antiviral signalling in humans. *Nature* **560**, 238–242
3. Hooftman, A., Peace, C. G., Ryan, D. G., Day, E. A., Yang, M., McGettrick, A. F., *et al.* (2023) Macrophage fumarate hydratase restrains mtrna-mediated interferon production. *Nature* **615**, 490–498
4. Becker, Y. L. C., Duvvuri, B., Fortin, P. R., Lood, C., and Boilard, E. (2022) The role of mitochondria in rheumatic diseases. *Nat. Rev. Rheumatol.* **18**, 621–640
5. Riley, J. S., and Tait, S. W. G. (2020) Mitochondrial DNA in inflammation and immunity. *EMBO Rep.* **21**, e49799
6. Yoon, J., Lee, M., Ali, A. A., Oh, Y. R., Choi, Y. S., Kim, S., *et al.* (2022) Mitochondrial double-stranded RNAs as a pivotal mediator in the pathogenesis of sjögren's syndrome. *Mol. Ther. Nucleic Acids* **30**, 257–269
7. Caielli, S., Wan, Z., and Pascual, V. (2023) Systemic lupus erythematosus pathogenesis: interferon and beyond. *Ann. Rev. Immunol.* **41**, 533–560
8. Buang, N., Tapeng, L., Gray, V., Sardini, A., Whilding, C., Lightstone, L., *et al.* (2021) Type i interferons affect the metabolic fitness of CD8+ t cells from patients with systemic lupus erythematosus. *Nat. Commun.* **12**, 1980
9. Lee, H. M., Sugino, H., Aoki, C., and Nishimoto, N. (2011) Underexpression of mitochondrial-DNA encoded atp synthesis-related genes and DNA repair genes in systemic lupus erythematosus. *Arthritis Res. Ther.* **13**, R63
10. Lewis, J. A., Huq, A., and Najarro, P. (1996) Inhibition of mitochondrial function by interferon. *J. Biol. Chem.* **271**, 13184–13190
11. Lou, J., Anderson, S. L., Xing, L., and Rubin, B. Y. (1994) Suppression of mitochondrial messenger-rna levels and mitochondrial-function in cells

responding to the anticellular action of interferon. *J. Interferon Res.* **14**, 33–40
12. Schneider, W. M., Chevillotte, M. D., and Rice, C. M. (2014) Interferon-stimulated genes: a complex web of host defenses. *Ann. Rev. Immunol.* **32**, 513–545
13. Seo, J.-Y., Yaneva, R., and Cresswell, P. (2011) Viperin: a multifunctional, interferon-inducible protein that regulates virus replication. *Cell Host Microbe* **10**, 534–539
14. Ghosh, S., and Marsh, E. N. G. (2020) Viperin: an ancient radical sam enzyme finds its place in modern cellular metabolism and innate immunity. *J. Biol. Chem.* **295**, 11513–11528
15. Landgraf, B. J., McCarthy, E. L., and Booker, S. J. (2016) Radical s-adenosylmethionine enzymes in human health and disease. *Ann. Rev. Biochem.* **85**, 485–514
16. Baker, E. P., and Barber, M. F. (2020) Unearthing the ancient origins of antiviral immunity. *Cell Host Microbe* **28**, 629–631
17. Gizzi, A. S., Grove, T. L., Arnold, J. J., Jose, J., Jangra, R. K., Garforth, S. J., *et al.* (2018) A naturally occurring antiviral ribonucleotide encoded by the human genome. *Nature* **558**, 610–614
18. Crosse, K. M., Monson, E. A., Beard, M. R., and Helbig, K. J. (2018) Interferon-stimulated genes as enhancers of antiviral innate immune signaling. *J. Innate Immun.* **10**, 85–93
19. Chen, S. Y., Ye, J. N., Lin, Y. F., Chen, W. X., Huang, S. H., Yang, Q. R., *et al.* (2024) Crucial roles of *RSAD2*/viperin in immunomodulation, mitochondrial metabolism and autoimmune diseases. *Inflammation*. https://doi.org/10.1007/s10753-024-02076-5
20. Chin, K. C., and Cresswell, P. (2001) Viperin (cig5), an ifn-inducible antiviral protein directly induced by human cytomegalovirus. *Proc. Natl. Acad. Sci. USA* **98**, 15125–15130
21. Xin, Y., He, Z. H., Mei, Y., Li, X., Zhao, Z. D., Zhao, M. M., *et al.* (2023) Interferon-α regulates abnormally increased expression of *RSAD2* in Th17 and Tfh cells in systemic lupus erythematosus patients. *Eur. J. Immunol.* **53**, e2350420
22. Choi, K. M., Kim, J. J., Yoo, J., Kim, K. S., Gu, Y. E., Eom, J., *et al.* (2022) The interferon-inducible protein viperin controls cancer metabolic reprogramming to enhance cancer progression. *J. Clin. Invest.* **132**, e157302
23. Taanman, J. W. (1999) The mitochondrial genome: Structure, transcription, translation and replication. *Biochim. Biophys. Acta* **1410**, 103–123
24. Tan, B. G., Gustafsson, C. M., and Falkenberg, M. (2024) Mechanisms and regulation of human mitochondrial transcription. *Nat. Rev. Mol. Cell Biol.* **25**, 119–132
25. Rackham, O., and Filipovska, A. (2022) Organization and expression of the mammalian mitochondrial genome. *Nat. Rev. Genet.* **23**, 606–623
26. McShane, E., Couvillion, M., Ietswaart, R., Prakash, G., Smalec, B. M., Soto, I., *et al.* (2024) A kinetic dichotomy between mitochondrial and nuclear gene expression processes. *Mol. Cell* **84**, 1541–1555
27. Moran, J. C., Brivanlou, A., Brischigliaro, M., Fontanesi, F., Rouskin, S., and Barrientos, A. (2024) The human mitochondrial mRNA structurome reveals mechanisms of gene expression. *Science* **385**, eadm9238
28. Ringel, R., Sologub, M., Morozov, Y. I., Litonin, D., Cramer, P., and Temiakov, D. (2011) Structure of human mitochondrial RNA polymerase. *Nature* **478**, 269–273
29. Arnold, J. J., Smidansky, E. D., Moustafa, I. M., and Cameron, C. E. (2012) Human mitochondrial RNA polymerase: Structure-function, mechanism and inhibition. *Biochim. Biophys. Acta* **1819**, 948–960
30. Lee, J. H., Wood, J. M., Almo, S. C., Evans, G. B., Harris, L. D., and Grove, T. L. (2023) Chemoenzymatic synthesis of 3'-deoxy-3',4'-didehydro-cytidine triphosphate (ddhCTP). *ACS Bio Med. Chem. Au* **3**, 322–326
31. Hsieh, A. H., Reardon, S. D., Munozvilla-Cabellon, J. H., Shen, J., Patel, S. S., and Mishanina, T. V. (2023) Expression and purification of recombinant human mitochondrial rna polymerase (POLRMT) and the initiation factors TFAM and TFB2M. *Bio. Proto.c* **13**, e4892
32. Smidansky, E. D. A.,J. J., Reynolds, S. L., and Cameron, C. E. (2011) Human mitochondrial rna polymerase: Evaluation of the single-nucleotide-addition cycle on synthetic RNA/DNA scaffolds. *Biochemistry* **50**, 5016–5032
33. Hsu, J. C. C., Laurent-Rolle, M., Pawlak, J. B., Xia, H. J., Kunte, A., Hee, J. S., *et al.* (2022) Viperin triggers ribosome collision-dependent translation inhibition to restrict viral replication. *Mol. Cell* **82**, 1631–1636
34. Sologub, M., Litonin, D., Anikin, M., Mustaev, A., and Temiakov, D. (2009) Tfb2 is a transient component of the catalytic site of the human mitochondrial RNA polymerase. *Cell* **139**, 934–944
35. Bernheim, A., Millman, A., Ofir, G., Meitav, G., Avraham, C., Shomar, H., *et al.* (2021) Prokaryotic viperins produce diverse antiviral molecules. *Nature* **589**, 120–124
36. Bonekamp, N. A., Peter, B., Hillen, H. S., Felser, A., Bergbrede, T., Choidas, A., *et al.* (2020) Small-molecule inhibitors of human mitochondrial DNA transcription. *Nature* **588**, 712–717
37. Helbig, K. J., and Beard, M. R. (2014) The role of viperin in the innate antiviral response. *J. Mol. Biol.* **426**, 1210–1219
38. Wu, C. C. C., Peterson, A., Zinshteyn, B., Regot, S., and Green, R. (2020) Ribosome collisions trigger general stress responses to regulate cell fate. *Cell* **182**, 404–409
39. Schwinghammer, K., Cheung, A. C. M., Morozov, Y. I., Agaronyan, K., Temiakov, D., and Cramer, P. (2013) Structure of human mitochondrial RNA polymerase elongation complex. *Nat. Struct. Mol. Biol.* **20**, 1298
40. Leão, P., Little, M. E., Appler, K. E., Sahaya, D., Aguilar-Pine, E., Currie, K., *et al.* (2024) Asgard archaea defense systems and their roles in the origin of eukaryotic immunity. *Nat. Commun.* **15**, 6386
41. Seo, J.-Y., Yaneva, R., Hinson, E. R., and Cresswell, P. (2011) Human cytomegalovirus directly induces the antiviral protein viperin to enhance infectivity. *Science* **332**, 1093–1097
42. Dumbrepatil, A. B., Zegalia, K. A., Sajja, K., Kennedy, R. T., and Marsh, E. N. G. (2020) Targeting viperin to the mitochondrion inhibits the thiolase activity of the trifunctional enzyme complex. *J. Biol. Chem.* **296**, 2839–2849
43. Eom, J., Kim, J. J., Yoon, S. G., Jeong, H., Son, S., Lee, J. B., *et al.* (2019) Intrinsic expression of viperin regulates thermogenesis in adipose tissues. *Proc. Natl. Acad. Sc.* **116**, 17419
44. Weinstein, A. G., Godet, I., and Gilkes, D. M. (2022) The rise of viperin: the emerging role of viperin in cancer progression. *J. Clin. Invest.* **132**, e165907
45. Fitzgerald, K. A. (2011) The interferon inducible gene: viperin. *J. Interferon Cytokine Res.* **31**, 131–135
46. Vaupel, P., and Multhoff, G. (2021) Revisiting the warburg effect: Historical dogma versus current understanding. *J. Physiol.-London* **599**, 1745–1757
47. Bürkner, P. C. (2017) Brms: an R package for Bayesian multilevel models using Stan. *J. Stat. Softw.* **80**, 1–28
48. Kass, R. E., and Raftery, A. E. (1995) Bayes factors. *J. Am. Stat. Assoc.* **90**, 791–798